ECS Transactions, 61 (7) 113-121 (2014)
10.1149/06107.0113ecst ©The Electrochemical Society

Molecules in Circuits: a New Type of Microelectronics?

R. McCreery, A. Bergren, S. Nagy, H. Yan, A. Bayat, and M. Kondratenko

Department of Chemistry, University of Alberta, Alberta, T6G 2M9, Canada

We use surface chemistry, spectroscopy, and conjugated organic molecules to make "molecular junctions" consisting of a single layer of molecules a few nanometers thick between conducting carbon and copper electrodes, then we study the behavior of molecules as circuit elements. The primary goal is to design and build functional molecular electronic components to greatly enhance the already powerful world of silicon microelectronics.

Introduction

Molecules may be considered electronic systems, with electrons rapidly moving through orbitals within molecules and also long distances in biological metabolism and photosynthesis. The prospect of incorporating molecules into microelectronic circuits based on silicon and metallic conductors has great potential for enhancing consumer electronics, providing solar energy conversion, and permitting new functions not possible with silicon. In order to combine the electronic properties of molecules with conventional microelectronics, we need to understand how to "connect" to molecules as well as how electrons are transported through molecules. Once the "rules" of charge transport through molecules are understood, it should be possible to "rationally design" new molecular electronic devices for valuable functions not currently possible with silicon. While Molecular Electronics holds great promise, it also presents significant challenges in handling and fabrication of devices with dimensions of only a few nanometers.

"Molecular electronics" emerged in the past decade as the study of how electrons are transported through molecules(1-6), and is distinguished from "organic electronics" by the short transport distances involved(7). Existing organic field effect transistors and light emitting diodes generally involve organic layers much thicker than 10 nm, often up to more than 1000 nm, while molecular electronic devices are based on either single molecules or molecular layers with thicknesses of 1-20 nm. In this short distance regime, unusual transport modes such as tunneling and field ionization become possible, and novel electronic behaviors are anticipated. An attractive goal of molecular electronics is demonstration of the effect of molecular structure on electronic behavior, since there is a wide variety of molecules available, and it should be possible to "tune" electronic properties by variations in structure. Ultimately, it may be possible to "rationally design" electronic devices with functions and behaviors not currently possible with silicon or other conventional semiconductors. The basic subunit of molecular electronics is the "molecular junction" (MJ), an example of which is shown in figure 1A. "Two terminal" MJs consist of a single molecule or a <10 nm layer of molecules between conducting contacts, such that the molecule(s) become circuit elements, possibly combined with conventional components in a "hybrid" microelectronic device.

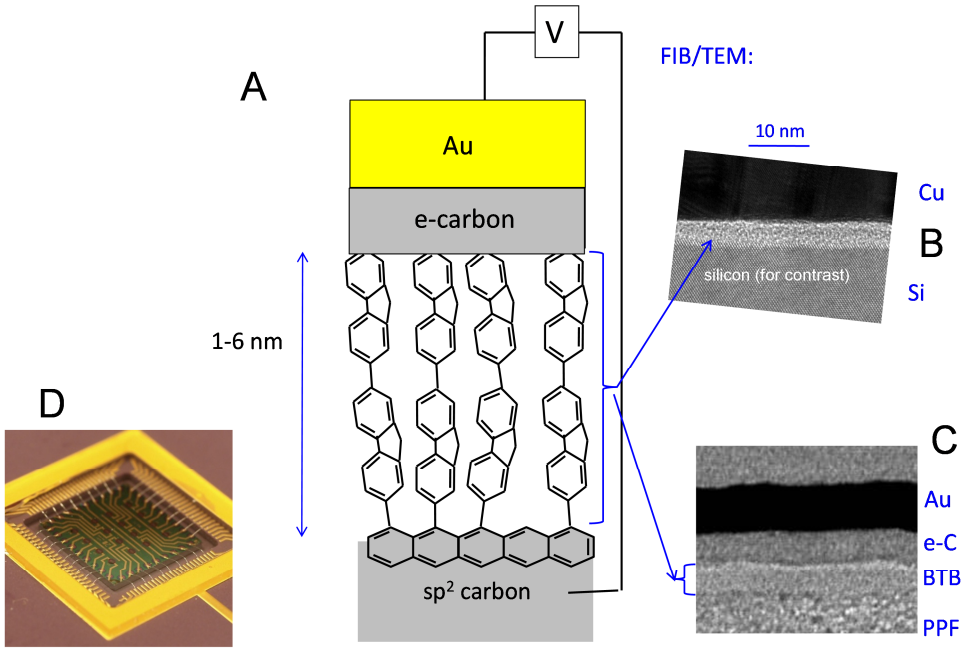

Figure 1. A) Schematic of 2-terminal molecular junction, with a bilayer of fluorene molecules. B) Focused ion-beam/TEM cross section of silicon/nitroazobenzene/Cu MJ; C) Cross section of PPF/BTB/e-C/Au MJ; D. packaged "chip" of MJs, with wire bonding between a commercial package and pads on the MJ surface.

Fabrication and Analysis

There have been a wide range of MJs reported in the literature, but this report is focussed on those containing sp^2 hybridized carbon as one or both of the "contacts" in the MJ. As is well known, carbon is unique in its electronic properties, exhibiting both metallic conduction and the ability to covalently bond to a variety of other materials and organic molecules (8). In particular, graphitic carbon forms covalent, conjugated bonds with aromatic molecules which result from electrochemical reduction of aryl diazonium reagents (8-10). As will be described below, this bonding results in strong electronic coupling between the carbon contact and the molecular layer which has significant consequences to electronic behavior (11). The carbon substrate has been described previously, and is designated "pyrolyzed photoresist film" (PPF) (12-14), shown in figure 2A.

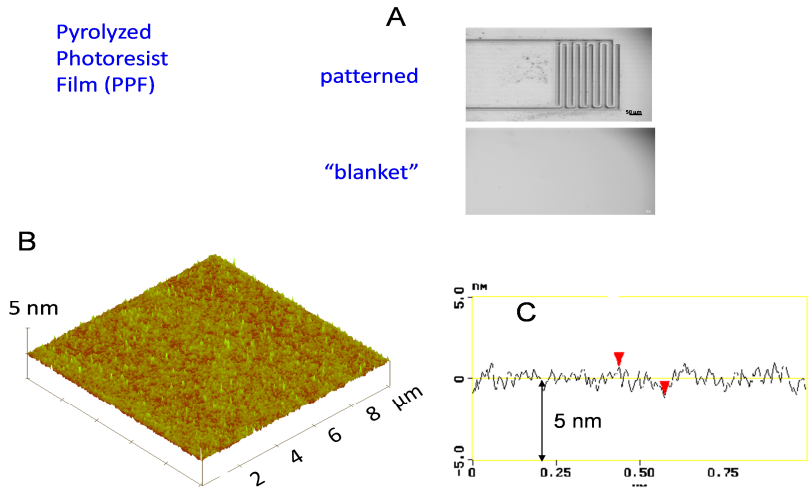

Figure 2. A) Images of patterned and blanket PPF. B) AFM or 10x10 um section of PPF surface. C) Line scan along a 1 μm line on PPF, showing an rms roughness of <0.5 nm.

Pyrolysis of conventional photoresist in a reducing atmosphere leads to a very flat but disordered sp^2 carbon surface, which may be patterned by photolithography prior to pyrolysis. The surface has a root mean square roughness below 0.5 nm (shown in fig 2B and C), which is essential for making devices with molecular layers a few nm thick (15). Deposition of the molecular layer by reduction of diazonium ions followed by AFM "scratching" to verify the layer thickness results in a modified PPF surface suitable for vapor deposition of a top contact by electron-beam evaporation (16-18). Figure 1B shows a TEM cross section of a PPF/nitroazobenzene/Cu MJ after deposition of Cu and a focussed ion beam sectioning, and 1C shows a similar junction using e-beam carbon as the top contact. Note that the molecules are not resolved in these images, but it is clear that the interfaces on both sides of a ~3 nm thick molecular layer are well resolved and reasonably uniform. Many details about MJ fabrication on PPF/molecular layers have been published elsewhere (4, 5, 19-21).

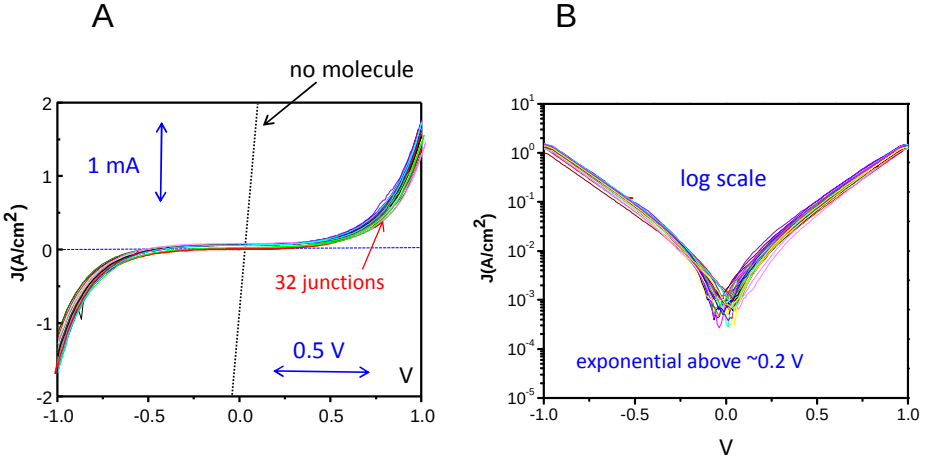

Figure 3. A) Overlay of JV curves from 32 molecular junctions (80 x 80 um) with a 3.8 nm multilayer of nitroazobenzene between carbon and Cu. Dotted line is for an identical device lacking the NAB layer. B) Same data on a logarithmic axis. Adapted with modifications from reference(22) .

Overlays of current density (J) vs bias voltage (V) curves for 32 molecular junctions containing a 3.8 nm thick layer of nitroazobenzene (NAB) are shown in figure 3A, and the corresponding ln(J) vs. V plot is shown in 3B (22). The JV curves are independent of scan rate over a wide range, and the exponential increase of current with bias voltage is consistent with charge transport by tunneling. Activated events such as redox exchange are ruled out by the very weak temperature dependence, with no change in the JV curves between 5 K and 250K. As shown in figure 4, the current density at a particular bias (0.1 V in this case) decreases exponentially with molecular layer thickness, also consistent with tunneling transport.

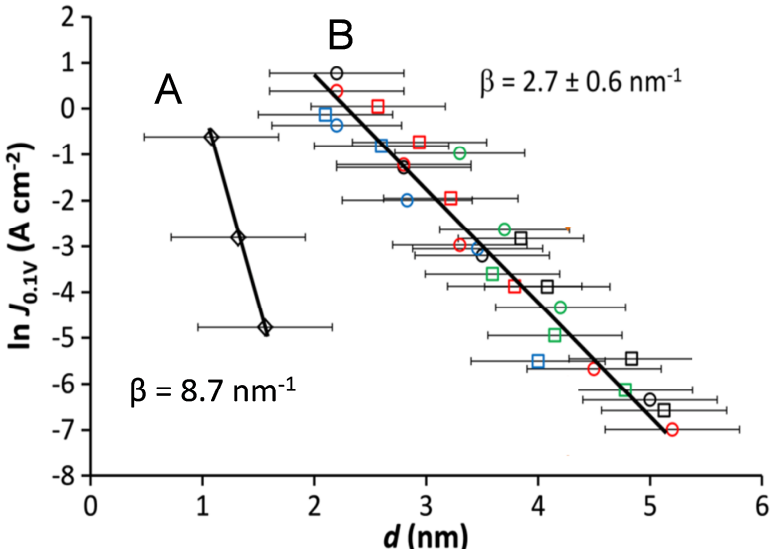

Figure 4. Natural logarithm of current density at a bias of 0.1 V plotted vs. the molecular layer thickness for nine molecules and a a total of >400 molecular junctions. Error bars are in the thickness measurement, and error bars for current density of > 4 molecular junctions are smaller than the points shown. Lines are least squares fits to data for aliphatic (line A) and aromatic (B) junctions, with their slopes indicated (β). Adapted with modifications from reference (11).

Curve A is for aliphatic molecular layers, with curve B is for eight different aromatic molecules with Cu as the top contact. Note that the slope of 8.7 nm^{-1} for alkanes is quite similar to the 6-9 nm range observed for transport through alkane layers in a variety of molecular junctions as well as for electron transfer to molecules in electrolyte solution(19). The lower slope of 2.7 nm^{-1} observed for aromatic molecules indicates that transport is significantly more efficient through conjugated structures, also consistent with other observations. However, the various aromatic molecules are not statistically different from each other, despite significant variations in their molecular orbital energies. This result was unexpected, but eventually explained by strong electronic coupling between the molecule and PPF, which affects both the apparent PPF work function as well as the molecular energy levels. The resulting "leveling effect" compresses the expected tunneling barriers to a similar value of 1.3 ± 0.2 eV, as is reflected in both the transport measurements and independent confirmation with photoelectron spectroscopy (11). A visual depiction of such electronic coupling is shown in figure 5, calculated for a model system of a 9-ring graphene "electrode" bonded to a NAB molecule. The orbital shown is the most likely to be involved in tunneling transport, and it is clear that it has density on both the"electrode" and the NAB. Such

coupling is a direct consequence of the conjugated, covalent bond between the aromatic PPF lattice and the aromatic molecules, and may therefore be unique to carbon-based molecular junctions.

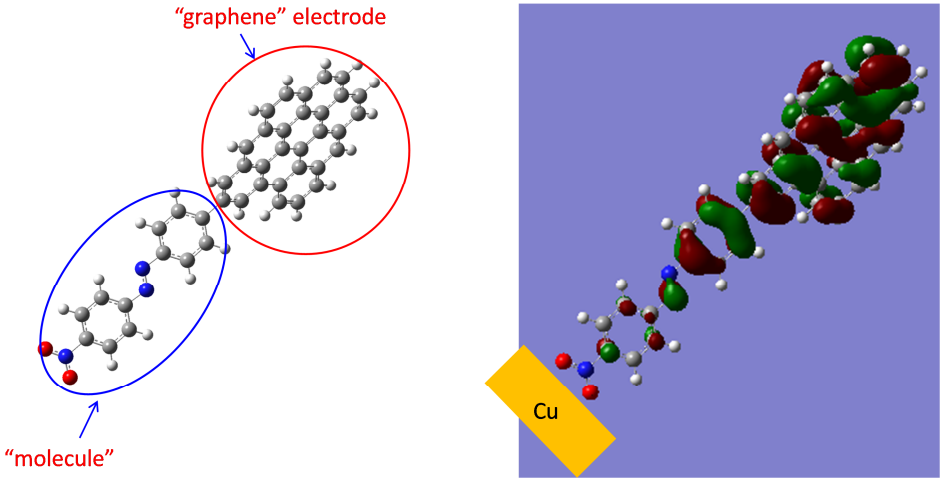

Figure 5. Model structure of NAB bonded to the edge of a 9-ring graphene fragment representing the sp^2 carbon electrode (left). At the right is the HOMO-1 orbital likely to be involved in transport calculated with density functional theory (B3LYP-6-31g (d)), showing that it has electron density on both the graphene and NAB.

The levelling effect apparent in figure 4B at least partially frustrates attempts to vary electronic characteristics by modify structure, although does not rule out structural control by more dramatic changes in molecular structure. In order to explore thicker junctions and higher bias voltages, we developed e-beam deposited carbon (e-C) as a top electrode. One advantage of e-C is shown in figure 6, which compares PPF/NAB/Cu/Au to PPF/NAB/e-C/Au devices having the same NAB thickness.

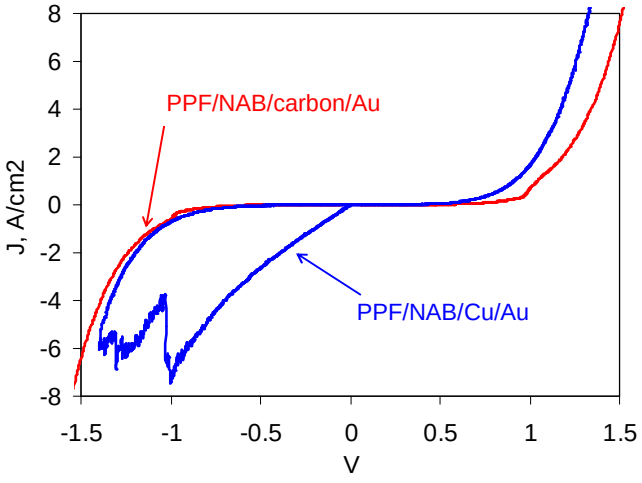

Figure 6. JV curves for the indicated MJs, both with equal thickness of NAB. Scans were started in positive direction, reversed at +1.5 V, then reversed again at -1.5 V. Cu is positively biased when -1.5 V is imposed, causing oxidation and migration of Cu into the molecular layer. See original papers for details (23, 24).

At sufficient negative bias, the positively bias Cu electrode oxidizes and permeates the molecular layer, thus forming Cu filaments which directly connect the PPF and Cu

electrodes(23). Since e-C is much less prone to oxidation or electromigration than Cu, and it becomes possible to scan "all-carbon" MJs to at least ±6 V bias. In addition, e-C is much less likely to penetrate the molecular layer during deposition, since carbon atoms and clusters are less prone to diffusion than metal atoms. As already noted in figure 1C, a FIB/TEM cross section of a PPF/molecule/e-C/Au molecular junction exhibits distinct interfaces between each layer, and also provides an independent determination of layer thicknesses to confirm the "standard" AFM measurements.

All carbon junctions were constructed from bis-thienyl-benzene (BTB) layers for a wide range of thickness (4.5- 22 nm) in order to extend transport measurements beyond the tunneling range shown in figure 4. BTB has been studied in detail as an electrode modification, and carbon/BTB electrodes show unusual electrochemical effects, such as rectification and conductance switching. JV curves for PPF/BTB/e-C/Au MJs are shown in figure 7 for eight different BTB thicknesses on a linear (7A) and natural log (7B) scale, all at room temperature.

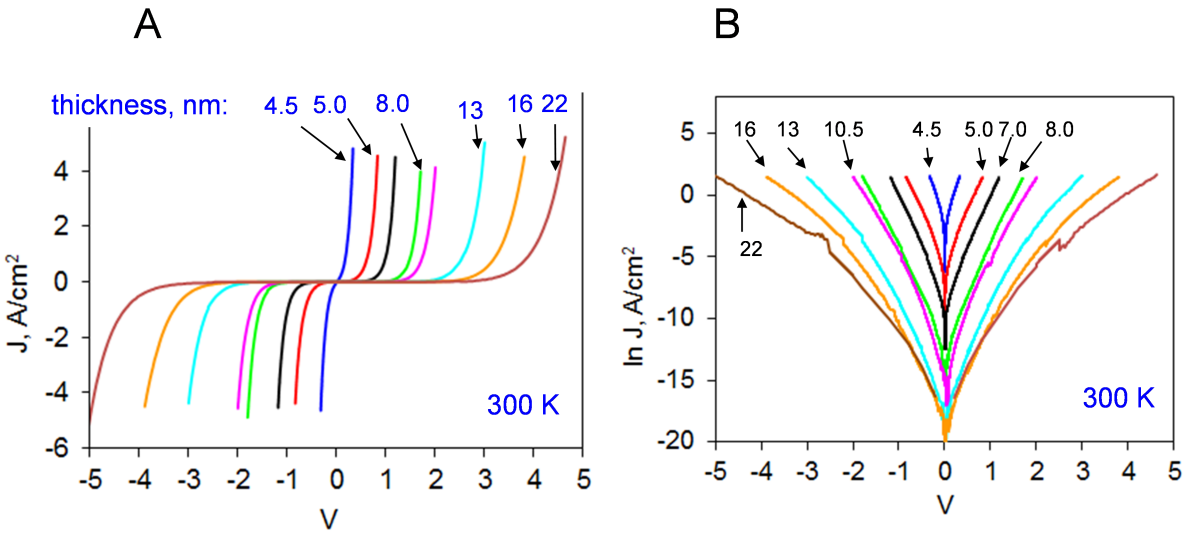

Figure 7. JV curves for the indicated PPF/BTB/e-C/Au MJs, with the indicated BTB layer thicknesses (all in nm) at room temperature, on a linear (A) and logarithmic (B) current density axis. Adapted with modifications from reference(21).

Note first that high current densities are observed through 22 nm thick BTB layers, which are much too thick for conventional (i.e. "coherent") tunneling. The lnJ vs V plots for thicknesses above ~10 nm are not linear, indicating are more complex voltage dependence than the exponential behavior observed for thinner devices. Determination of the transport mechanism is aided by attenuation plots similar to figure 4, but over the wider thickness range available with BTB. An example for a bias of 1 V is shown in figure 8, over a wide temperature range (6K – 300K). Statistical analysis reveals three linear regions, implying at least three distinct transport mechanisms(21). For thickness (d) below 8 nm, a slope of ~3.0 nm^{-1} is observed, similar to that for the aromatic/Cu devices of figure 4. For d>12 nm, the slope is near zero above 250 K, but approached the 3.0 nm^{-1} line at low T.

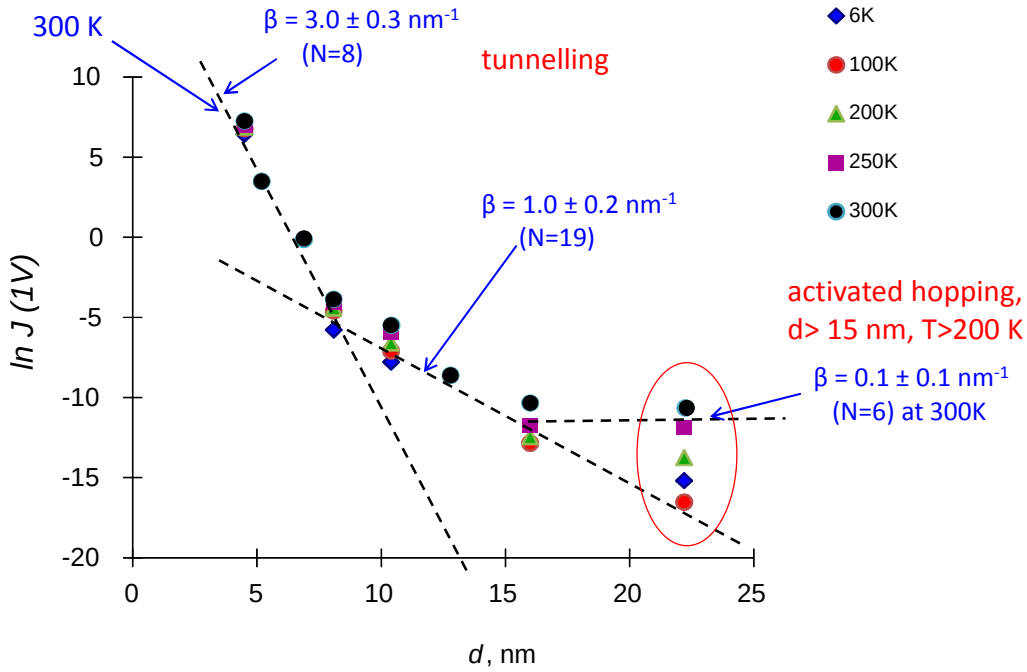

Figure 8. Natural log of current density at 1 V bias for PPF/BTB/e-C/Au MJs are various temperatures between 6 and 300 K. Only the thickest MJs indicated activation energy above 100 meV. See reference(21) for details.

The Arrhenius slope above 250 K is 160 meV, similar to "hopping" transport observed In bulk polythionene. This result is consistent with hopping mechanism mediated by redox exchange, with the expected weak dependence on layer thickness. The slope for d=8-12 nm is 1.0 ±0.2 nm^{-1}, and this line is extended to >15 nm thicknesses for low T. We proposed one possibility of the 1.0 nm^{-1} slope region based on field ionization of the HOMO level of BTB, to generate free carriers and possibly conducting BTB polarons(21). There are other possibilities, but whatever mechanism is proposed, it must exhibit linearity of ln(J/E) vs $E^{1/2}$ linearity over 8 orders of magnitude of current at < 10K.

The results to date enable some rational changes in molecular structure which should have major effects on transport. Such changes are expected in the thickness regime above ~7 nm, where the "leveling" effect of strong coupling is less important. Modifications presented at the meeting include removal moving the HOMO closer to the Fermi level using a ferrocene derivative, removal of one thiophene ring from BTB, and incorporation of an electron acceptor into films in the range of 7-25 nm thickness. When operating in this range, molecular structure has a much stronger effect on conduction than that in the tunneling regime.

Conclusions

In closing, we note several distinct properties of sp^2 carbon as a component of electronic devices which incorporate molecules as active components. First, the conjugated. covalent bond between an sp^2 carbon substrate and an aromatic molecular results in strong electronic coupling which significantly perturbs the electronic properties of the individual components(11). Such coupling may also occur between metals and

aromatic molecules, but its effects on electronic behavior are not yet apparent(25). Second, the C-C bond between PPF and the aromatic molecules is thermally quite stable, permitting temperature excursions from 5K to >600K without significant changes to junction properties(26). Many likely applications of MJs in microelectronics require elevated processing and operating temperatures, so thermal stability is important. Third, sp^2 carbon is not subject to electromigration, unlike many metals, notably Ag, Au, and Cu. The "all-carbon" molecular junctions may be able to tolerate much higher local current densities as a result. Finally, the ability to covalently modify sp^2 carbon surfaces with a variety of molecules with a range of chemical and electronic properties permits exploration of many phenomena and properties very distinct from those of conventional electronic materials, thus aiding the goal of achieving electronic functions difficult or impossible to achieve with silicon, such as lower cost, low power consumption, chemical sensing and mechanical flexibility.

Acknowledgments

The work described in this paper was supported by the National Research Council, the Natural Science and Engineering Research Council, and the Government of Alberta.

References

1. J. Jortner and M. Ratner, *Molecular Electronics*, p. 485, Blackwell Science Ltd. (1997).
2. B. Kim, J. M. Beebe, Y. Jun, X. Y. Zhu and C. D. Frisbie, *J. Am. Chem. Soc.*, **128**, 4970 (2006).
3. S. M. Lindsay and M. A. Ratner, *Adv. Mater.*, **19**, 23 (2007).
4. R. McCreery, *Chem. Mat.*, **16**, 4477 (2004).
5. R. McCreery, J. Wu and R. J. Kalakodimi, *Phys. Chem. Chem. Physics.*, **8**, 2572 (2006).
6. N. J. Tao, *Nat Nanotech*, **1**, 173 (2006).
7. R. McCreery, H. Yan and A. J. Bergren, *Phys. Chem. Chem. Phys.*, **15**, 1065 (2013).
8. R. L. McCreery, *Cheml Rev*, **108**, 2646 (2008).
9. D. Belanger and J. Pinson, *Chem Soc Rev*, **40**, 3995 (2011).
10. J. Pinson and F. Podvorica, *Chem Soc Rev*, **34**, 429 (2005).
11. S. Y. Sayed, J. A. Fereiro, H. Yan, R. L. McCreery and A. J. Bergren, *P Natl Acad Sci*, **109**, 11498 (2012).
12. R. Kostecki, X. Song and K. Kinoshita, *Electrochem Solid St*, **2**, 465 (1999).
13. S. Ranganathan and R. L. McCreery, *Anal. Chem.*, **73**, 893 (2001).
14. S. Ranganathan, R. L. McCreery, S. M. Majji and M. Madou, *J. Electrochem. Soc.*, **147**, 277 (2000).
15. F. Anariba, S. H. DuVall and R. L. McCreery, *Anal. Chem.*, **75**, 3837 (2003).
16. F. Anariba, J. Steach and R. McCreery, *J. Phys. Chem B*, **109**, 11163 (2005).
17. A. J. Bergren, K. D. Harris, F. Deng and R. L. McCreery, *J. Phys. Condens. Matter*, **20**, 374117 (2008).
18. A. J. Bergren, R. L. McCreery, S. R. Stoyanov, S. Gusarov and A. Kovalenko, *J. Phys. Chem. C*, **114**, 15806 (2010).
19. R. L. McCreery and A. J. Bergren, *Adv. Mater.*, **21**, 4303 (2009).
20. R. L. McCreery, U. Viswanathan, R. P. Kalakodimi and A. M. Nowak, *Faraday Discuss*, **131**, 33 (2006).

21. H. Yan, A. J. Bergren, R. McCreery, M. L. Della Rocca, P. Martin, P. Lafarge and J. C. Lacroix, *P Natl Acad Sci*, **110**, 5326 (2013).
22. J. Ru, B. Szeto, A. Bonifas and R. L. McCreery, *ACS Appl Mater Interfaces*, **2**, 3693 (2010).
23. S. Ssenyange, H. Yan and R. L. McCreery, *Langmuir*, **22**, 10689 (2006).
24. H. Yan, A. J. Bergren and R. L. McCreery, *J. Am. Chem. Soc.*, **133**, 19168 (2011).
25. B. Kim, S. H. Choi, X. Y. Zhu and C. D. Frisbie, *J. Am. Chem. Soc.*, **133**, 19864 (2011).
26. A. M. Mahmoud, A. J. Bergren, N. Pekas and R. L. McCreery, *Adv. Funct. Mater.*, **21**, 2273 (2011).